



Improved preparation technology of color-tunable long afterglow phosphors $\text{Sr}_{1.94-x}\text{Ca}_x\text{MgSi}_2\text{O}_7: \text{Eu}_{0.01}^{2+}, \text{Dy}_{0.05}^{3+}$

Chi Zhang, Chaoyong Deng*



Key Laboratory of Electronic Functional Composite Materials of Guizhou Province, Department of Electronic Science, College of Big Data and Information Engineering, Guizhou University, Guiyang, Guizhou 550025, PR China

ARTICLE INFO

Keywords:

Silicate
Sintering temperature
Luminescence
Long afterglow

ABSTRACT

Tetragonal long afterglow silicates, $\text{Sr}_{1.94-x}\text{Ca}_x\text{MgSi}_2\text{O}_7: \text{Eu}_{0.01}^{2+}, \text{Dy}_{0.05}^{3+}$ ($x=0, 0.388, 0.776, 1.164, 1.552, 1.94$), are successfully synthesized by high-temperature solid-state reaction at 1300 °C and 1350 °C, respectively. Addition of excess silicon dioxide can reduce the sintering temperature from 1350 °C to 1300 °C, and photoluminescence performances and afterglow properties are improved. All samples have the same tetragonal structure, but the diffraction peaks shift to higher angles when smaller Ca^{2+} ions gradually substitute Sr^{2+} sites in the host. The reduced interplanar spacing leads to increased crystal field strength. As a result, a red shift phenomenon is observed in the emission spectra with the increase of Ca^{2+} content. The afterglow emission bands also change from 466 to 529 nm when the proportion of Ca^{2+} ions increases in the host. Both luminescence and afterglow colors can continuously vary from blue to green by adjusting the Ca/Sr ratio in the host, and emission wavelength is linear with the concentration of Ca^{2+} (x). With increasing the concentration of Ca^{2+} , the thermal stability is improved and the quenching temperature increases, but the afterglow properties deteriorate.

1. Introduction

The long afterglow phosphors irradiated by sunlight or artificial light are able to absorb the energy and the luminescence will last for a long time after the removal of excitation [1,2]. The phosphor with persistent luminescence is a new kind of material for energy storage. These phosphors can store solar energy or other luminous energies which can be released as light in the dark. Consequently, the long afterglow phosphors are known as green luminescence materials and have received more and more attention in recent years because of their applications in weak-light illumination, solar energy utilization, information storage and in-vivo bio-imaging [3,4].

For the past few years, Eu^{2+} ions acting as luminescent centers have merited much attention due to their broad excitation and emission bands with high efficiency. The broadband emission of Eu^{2+} observed in many phosphors is caused by the $4f^7 (^8S_{7/2}) - 4f^6 5d^1$ transitions [5]. The 5d electrons located in the outer orbit and the energies are more dependent on the environment, so the wavelength positions of the emission bands can be tuned hinging on different environment in various hosts. A wide variety of materials have been used as the hosts for Eu^{2+} -doped phosphors, and silicates are the popular long afterglow host materials [6–10].

The emission spectra of the best known persistent luminescent

silicates, $\text{Sr}_2\text{MgSi}_2\text{O}_7: \text{Eu}^{2+}, \text{Dy}^{3+}$ and $\text{Ca}_2\text{MgSi}_2\text{O}_7: \text{Eu}^{2+}, \text{Dy}^{3+}$, are attributed to the transition from $4f^6 5d^1$ excited state to $4f^7$ ground state configuration of Eu^{2+} ions [11], and the emission bands are located in different positions owing to the impressionable 5d level. Hence, the emitting colors will be altered with increasing concentration of Ca^{2+} (x) in the $\text{Sr}_{2-x}\text{Ca}_x\text{MgSi}_2\text{O}_7: \text{Eu}^{2+}, \text{Dy}^{3+}$ phosphors. Because the synthesis temperatures for $\text{Sr}_2\text{MgSi}_2\text{O}_7$ and $\text{Ca}_2\text{MgSi}_2\text{O}_7$ are different, the $\text{Sr}_{2-x}\text{Ca}_x\text{MgSi}_2\text{O}_7: \text{Eu}^{2+}, \text{Dy}^{3+}$ long afterglow phosphors have been synthesized by solid-state reaction with different sintering temperatures [12] or by combustion method [13]. To the best of our knowledge, $\text{Sr}_{2-x}\text{Ca}_x\text{MgSi}_2\text{O}_7: \text{Eu}^{2+}, \text{Dy}^{3+}$ phosphors synthesized under the same sintering temperature have not been reported. According to the results of previous studies, adding excessive SiO_2 in the raw materials is useful for synthesizing a single akermanite phase at a reduced sintering temperature with improved luminescent properties. Thus, 20 and 30 mol% of SiO_2 are considered appropriate for $\text{Ca}_{1.94}\text{MgSi}_2\text{O}_7: \text{Eu}_{0.01}^{2+}, \text{Dy}_{0.05}^{3+}$ [14] and $\text{Sr}_{1.94}\text{MgSi}_2\text{O}_7: \text{Eu}_{0.01}^{2+}, \text{Dy}_{0.05}^{3+}$ sintered at 1300 °C, respectively. Therefore, excess SiO_2 is selected as additional materials to reduce the sintering temperature from 1350 °C to 1300 °C and improve luminescent properties of $\text{Sr}_{1.94-x}\text{Ca}_x\text{MgSi}_2\text{O}_7: \text{Eu}_{0.01}^{2+}, \text{Dy}_{0.05}^{3+}$.

In this paper, $\text{Sr}_{1.94-x}\text{Ca}_x\text{MgSi}_2\text{O}_7: \text{Eu}_{0.01}^{2+}, \text{Dy}_{0.05}^{3+}$ ($x=0, 0.388, 0.776, 1.164, 1.552, 1.94$) long afterglow phosphors were successfully prepared at 1300 °C and 1350 °C, respectively. The powder X-ray

* Corresponding author.

E-mail address: cydeng@gzu.edu.cn (C. Deng).

diffraction patterns, luminescence and long afterglow properties of $\text{Sr}_{1.94-x}\text{Ca}_x\text{MgSi}_2\text{O}_7: \text{Eu}_{0.01}^{2+}, \text{Dy}_{0.05}^{3+}$ ($x=0, 0.388, 0.776, 1.164, 1.552, 1.94$) were studied in detail. The emission color variation is presented in emission and afterglow emission spectra. The persistent luminescence mechanism is also discussed.

2. Materials synthesis and characterization

The $\text{Sr}_{1.94-x}\text{Ca}_x\text{MgSi}_2\text{O}_7: \text{Eu}_{0.01}^{2+}, \text{Dy}_{0.05}^{3+}$ ($x=0, 0.388, 0.776, 1.164, 1.552, 1.94$) samples were prepared by high temperature solid-state reaction method. SrCO_3 (AR) CaCO_3 (AR), MgO (AR), SiO_2 (3N), Eu_2O_3 (4N) and Dy_2O_3 (3N) were used as raw materials. Stoichiometric amounts of raw materials and a certain amount of additional SiO_2 were weighed and mixed thoroughly in an agate mortar. Then the pre-sintered powders were prepared at 800°C for 2 h in air atmosphere. After that, the powder mixtures were milled again and then pressed into tablets before sintered at 1300°C or 1350°C in a slightly reducing atmosphere of carbon monoxide for 4 h. The $\text{Sr}_{1.94-x}\text{Ca}_x\text{MgSi}_2\text{O}_7: \text{Eu}_{0.01}^{2+}, \text{Dy}_{0.05}^{3+}$ ($x=0, 0.388, 0.776, 1.164, 1.552, 1.94$) samples sintered at 1300°C were synthesized with 30, 28, 26, 24, 22 or 20 mol% additional SiO_2 , respectively. The samples sintered at 1350°C were synthesized without any additional materials. Finally, the samples $\text{Sr}_{1.94-x}\text{Ca}_x\text{MgSi}_2\text{O}_7: \text{Eu}_{0.01}^{2+}, \text{Dy}_{0.05}^{3+}$ ($x=0, 0.388, 0.776, 1.164, 1.552, 1.94$), denoted as SMSO, 20% Ca, 40% Ca, 60% Ca, 80% Ca and CMSO) were obtained.

Phase measurements of the synthesized samples were performed on a Rigaku Smartlab X-ray diffractometer (XRD) with $\text{Cu K}\alpha$ radiation at 40 kV tube voltage and 150 mA tube current. The room temperature excitation, photoluminescence and persistent luminescence spectra of all samples were recorded by HORIBA FluoroMax[®]-4 spectrofluorometer with a 150 W xenon lamp. The temperature dependent properties were examined by a variable temperature device measured from 25°C to 200°C . The decay curves were detected using the same spectrofluorometer. Prior to the measurement, the synthesized samples were irradiated by a 365 nm ultraviolet lamp for 30 min.

3. Results and discussion

3.1. Phase

Fig. 1(a) and (b) show the XRD patterns of samples $\text{Sr}_{1.94-x}\text{Ca}_x\text{MgSi}_2\text{O}_7: \text{Eu}_{0.01}^{2+}, \text{Dy}_{0.05}^{3+}$ sintered at 1300°C and 1350°C , respectively. The diffraction peaks of SMSO and CMSO were well indexed to the standard data reported in JCPDS files 75-1736 and 83-1815, respectively. This means that samples SMSO and CMSO have the same P-42₁m melilite-type tetragonal crystal structure [15,16]. Accordingly, the patterns of SMSO samples are similar to that of CMSO. However, there is a slight difference in the lattice constant. The substitution of smaller Ca^{2+} (0.112 nm) ions for Sr^{2+} (0.126 nm) sites in the host leads to a decrease of the interplanar spacing, and the diffraction peak positions slightly shift to higher angles with the increase of Ca^{2+} content (Table 1).

In the XRD patterns of samples sintered at 1350°C , $\text{Sr}_3\text{MgSi}_2\text{O}_8$ (indicated by “□”) and $\text{Ca}_3\text{MgSi}_2\text{O}_8$ (indicated by “◆”) were observed as impurity phases, which is caused by incomplete reaction. Due to the addition of SiO_2 , $\text{M}_3\text{MgSi}_2\text{O}_8$ ($M=\text{Ca}, \text{Sr}$) impurity phases no longer exist, and small amounts of CaSiO_3 (JCPDS Cards 19-0248, indicated by “*”) are observed in the XRD patterns of samples sintered at 1300°C . The addition of SiO_2 can increase the Si/O ratio under reducing atmosphere, which facilitates the transformation from $\text{M}_3\text{MgSi}_2\text{O}_8$ to $\text{M}_2\text{MgSi}_2\text{O}_7$ ($M=\text{Ca}, \text{Sr}$) and results in the formation of CaSiO_3 .

3.2. Photoluminescence

In order to investigate the luminescence properties of all samples, the photoluminescence excitation and emission spectra of $\text{Sr}_{1.94-x}$

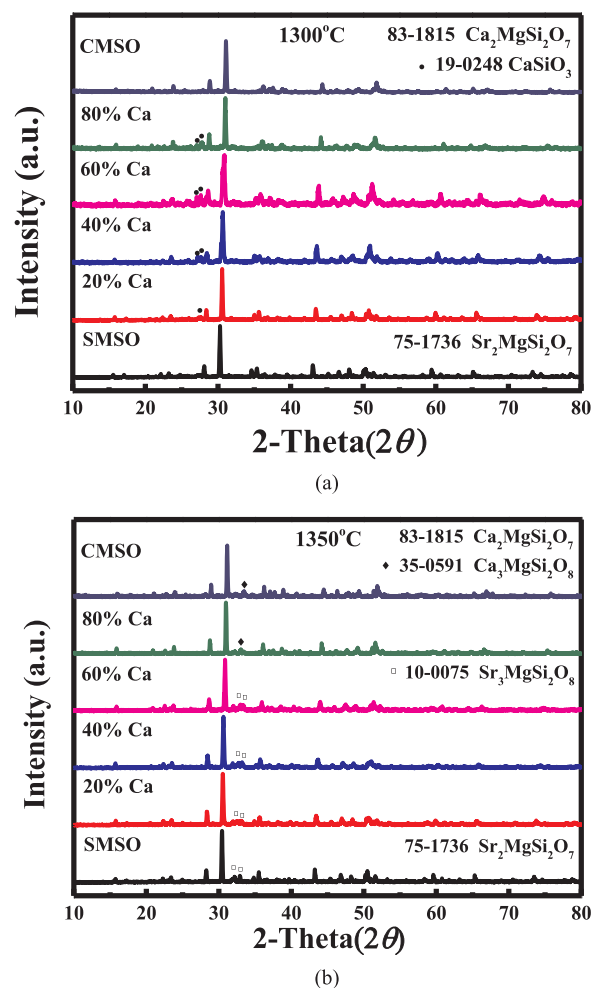


Fig. 1. (a) XRD patterns of $\text{Sr}_{1.94-x}\text{Ca}_x\text{MgSi}_2\text{O}_7: \text{Eu}_{0.01}^{2+}, \text{Dy}_{0.05}^{3+}$ ($x=0, 0.388, 0.776, 1.164, 1.552, 1.94$) sintered at 1300°C , (b) XRD patterns of $\text{Sr}_{1.94-x}\text{Ca}_x\text{MgSi}_2\text{O}_7: \text{Eu}_{0.01}^{2+}, \text{Dy}_{0.05}^{3+}$ ($x=0, 0.388, 0.776, 1.164, 1.552, 1.94$) sintered at 1350°C .

Table 1

The positions of the diffraction strongest peak of $\text{Sr}_{1.94-x}\text{Ca}_x\text{MgSi}_2\text{O}_7: \text{Eu}_{0.01}^{2+}, \text{Dy}_{0.05}^{3+}$ ($x=0, 0.388, 0.776, 1.164, 1.552, 1.94$).

	SMSO	20% Ca	40% Ca	60% Ca	80% Ca	CMSO
211 (2θ deg.)	30.28	30.58	30.66	30.89	31.02	31.10
1300 °C						
211 (2θ deg.)	30.44	30.56	30.64	30.88	31.02	31.16
1350 °C						

$\text{Ca}_x\text{MgSi}_2\text{O}_7: \text{Eu}_{0.01}^{2+}, \text{Dy}_{0.05}^{3+}$ ($x=0, 0.388, 0.776, 1.164, 1.552, 1.94$) sintered at 1300°C and 1350°C were measured. The left side of Fig. 2 shows the photoluminescence excitation spectra of samples from SMSO to CMSO. The excitation spectra of all samples were monitored at each emission peak. All the samples exhibit strong broad absorption band covering the region from ultraviolet to blue light. All excitation spectra of the samples are similar and the excitation peaks are located at 397 nm. Nevertheless, emission peaks at about 450, 462 and 467 nm become more and more obvious with the increase of Ca^{2+} content. That is to say, the samples can be efficiently excited by blue light when the Ca^{2+} content is greater than or equal to 60% ($x \geq 1.164$).

Emission spectra for samples SMSO to CMSO are shown in Fig. 2. All of the emission bands are ascribed to the electron transition from $4f^65d^1$ excited state to the $4f^7$ ($^8S_{7/2}$) ground state of the Eu^{2+} ions at room temperature. Compared with the emission spectra of samples prepared at 1300°C , the emission peaks of samples sintered at 1350°C shift to

Download English Version:

<https://daneshyari.com/en/article/5397404>

Download Persian Version:

<https://daneshyari.com/article/5397404>

[Daneshyari.com](https://daneshyari.com)